J Nanostruct 15(4): 2112-2117, Autumn 2025

RESEARCH PAPER

Gamma Ray Attenuation Using Nanocomposites for Multiple Radioactive Sources

Mohammed A. Mohmmed *, Anas A. Hamdi

Salahuddin Education Directorate, Ministry of Education, Salahuddin, Iraq

ARTICLE INFO

Article History:
Received 05 June 2025
Accepted 27 September 2025
Published 01 October 2025

Keywords:
Absorption coefficient
Cobalt ferrite
Epoxy
Geiger counter
Nanocomposites

ABSTRACT

Composites were prepared by dispersing 35 nm cobalt ferrite nanoparticles in a Bremer Epoxy resin (50/100) mixture. Various composites were formed using cobalt ferrite powder at 1 %–4 % wt. The specimens were prepared in the form of a cylindrical disc with different densities (15 mm). Density of individual samples have been calculated using dimensional analysis. Composites were screened using a Geiger counter. Mass attenuation reduction A key parameter in the study of how gamma rays interact with matter is mass attenuation. It represents the mass attenuation coefficient of gamma radiation by a material.

How to cite this article
Mohmmed M, Hamdi A. Gamma Ray Attenuation Using Nanocomposites for Multiple Radioactive Sources. J Nanostruct, 2025; 15(4):2112-2117. DOI: 10.22052/JNS.2025.04.051

INTRODUCTION

Finally, in order to enhance the accuracy of atomic and/or mass attenuation coefficient, a series of measurements were presented. The value of mass attenuation coefficient is not only important for the medical imaging systems, but also for the design of shielding materials against radiation [1]. Even though there are intriguing anecdotal evidence in this direction, in practice theory and experiment often have little to do with one another especially for novel or complex materials [2]. Such variations could lead to insufficient attenuation, or errors in image donation and highlight the need for regular validation of these data [3,4]. The gamma ray attenuation effect from sources such as Am-241, Cs-137, and Co-60 by this material of different densities had been reported previously in some other investigations [5, 6]. The main purpose of irradiating source samples [7] is to find the density (m) and m/ for each sample source. The low-density materials are proven to be effective in shielding the low ɣ emitters [8]. For high energy sources such as Co-60, it is required to use High Z or thick material with high mass density materials for efficient radiation shielding [9]. The mode should be extended to character formation in media with complex geometries, composites of materials58 different [10] for better prediction accuracy of the attenuation coefficients. This work could be a contribution in the literature as an investigation of scintillation properties of the material for gamma-ray absorption application. These results can be of interest in all the fields such as nuclear medicine, material science and radiotherapy [11]. The results may serve as a useful data for the researchers in the field of radiation

* Corresponding Author Email: Mohmmed.ab.mohmmed@st.tu.edu.iq

shielding, dosimeter, and simulation based on radiation physics. Efferent substances are essential in fields such as nuclear medicine, radiological safety, and industrial radiography. Owing to their high penetration capabilities, gamma rays interact through mechanisms such as the photoelectric effect, Compton scattering, and pair production.

Research Objectives:

1. To define and explain the mass attenuation coefficient in relation to gamma ray interactions with matter.

2. To review and analyze relevant experimental and theoretical studies involving various materials and their attenuation characteristics.

MATERIALS AND METHODS

Epoxy resin composites reinforced with 35 nm cobalt ferrite nanopowder were prepared by adding 1%–4% of cobalt ferrite powder to epoxy resin. Mechanical mixing and ultrasonic technology were applied to distribute the powder within the resin before adding the hardener. The mixture was poured into standard sample molds of 20 mm diameter and 15 mm thickness. A Geiger counter was used to calculate the linear absorption coefficient and mass absorption for all radioactive sources and the same sample. This device detects ionizing radiation, including gamma rays. Its working principle is based on the ionization of the gas inside the tube when exposed to radiation, resulting in an electrical pulse that can be detected and recorded. For the analysis of gamma ray attenuation, the device measures the radiation intensity before and after the radiation passes through a material. The attenuation rate μ is then calculated using appropriate equations [12]:

$$\mu = (1 / x) * \ln(I_o / I)$$

where: μ = linear attenuation coefficient, x = sample thickness, I_o = original intensity, I

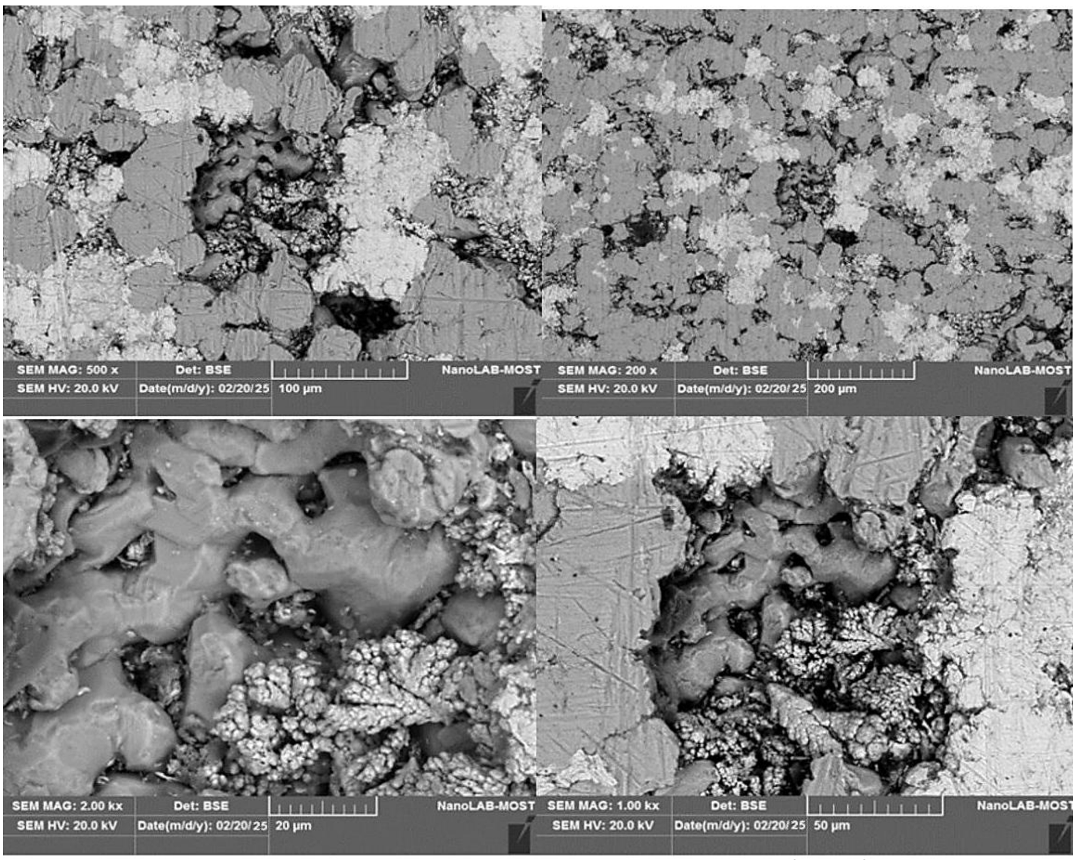

Fig. 1. The image in Figure 1 shows a scanning electron microscope examination of cobalt ferrite powder.

= measured radiation intensity after passing through the material.

RESULTS AND DISCUSSION

SEM analysis

The image in Fig. 1 shows a scanning electron microscope examination of cobalt ferrite powder. The Fig. 1 shows the presence of clusters and aggregates, the reason for which is due to the method of preparation. The figure also shows the overlap and regular distribution between the ferrite and cobalt, which gives the polymer magnetic properties and increases the magnetic susceptibility**.**

This study investigates the interaction between the gamma rays emitted by different radioactive sources (Am-241, Cs-137, and Co-60) and a shielding material of varying densities (Tables 1-3 and Fig. 1). The goal is to evaluate the linear attenuation coefficient (µ) and mass attenuation coefficient (µ/ρ) for each source and sample.

Linear Attenuation Coefficient (µ), Calculated as $\mu = 1/x \ln I_0 / I$

Am-241 (59.6 keV) is associated with the highest linear attenuation coefficient across all the samples. This is expected, as low-energy photons are likely to be absorbed or scattered by matter, leading to a high attenuation. Cs-137 (661.6 keV) is associated with moderate linear attenuation values. As the photon energy increases, the probability of interaction (especially photoelectric effect) decreases, thereby reducing the linear attenuation. Co-60 (1173 and 1332 keV) is associated with the lowest µ values. This finding is consistent with high-energy gamma rays having a low likelihood of interaction per unit distance in matter.

Mass Attenuation Coefficient (µ/ρ), Where ρ = density

The mass attenuation coefficient normalizes linear attenuation to the material's density for a comparison across different sample densities. While µ decreases with the increasing energy, µ/ρ emphasizes the difference in material effectiveness regardless of density [13]. µ/ρ shows a decreasing trend in the order of Am-241>Cs-137>Co-60, confirming the inverse relationship between photon energy and attenuation efficiency. This

Table 1. Results of Gamma Ray Attenuation by Nanocomposites Under Different Radiation Sources.

Sample Code	Am-241 59.6Kev	Cs-137 661.66 Kev	Co-60 1173.24Kev	Co-60 1332.3 Kev	Density g \ cm^3	Thickness X mm	Weight g
I_o	10787	6190	1173.24	1332.3			
Counts	I_{out}	I_{out}	I_{out}	I_{out}			
S_o	1419	2505	1059	902	1.24	15	4.8
S_1	1341	2395	1091	900	1.67	15	4.59
S_2	1341	2493	1066	883	189	15	4.26
S_3	1342	2312	1018	851	2.1	15	4.86
S_4	1235	2137	940	791	2.6	15	5.63

Table 2. Linear and Mass Attenuation Coefficients under Different Radioactive Sources.

Source	Energy (keV)	u (cm^-1)	u/rho (cm^2/g)
Am-241	59.6	1.352	1.09
Cs-137	661.66	0.602	0.485
Co-60	1173.24	0.069	0.056
Co-60	1332.3	0.26	0.21

trend aligns with the following well-established photon–matter interaction principles:

1- At low energies, the photoelectric effect dominates. This effect has a strong dependence on atomic number (Z) and results in high attenuation (as observed for Am-241).

2- At intermediate energies, Compton scattering is the primary mode of interaction, contributing moderately to attenuation (e.g., Cs-137).

3- At high energies, pair production becomes possible (above 1.022 MeV) but contributes less than the photoelectric effect and Compton scattering unless the material is extremely dense or thick, explaining the low μ for Co-60.

These findings confirm that for effective gamma shielding:

1- Low-energy gamma-ray sources require less dense material for significant attenuation.

2- High-energy gamma-ray sources such as Co-60 require materials with high Z and/or great thickness.

Table 3 shows the linear attenuation coefficient (u) and mass attenuation coefficient (u/rho) for each radioactive source and sample (S0–S4) based on experimental data. Sample S0 is considered the baseline sample with initial intensity measurements presented in [14]. Table 1 presents the linear (u) and mass attenuation coefficients

Table 3. Linear and Mass Attenuation Coefficients for Epoxy and Nanocomposites.

Sample	Density (g/cm³)	Am-241 (u / u/rho)	Cs-137 (u / u/rho)	Co-60 (1173) (u / u/rho)	Co-60 (1332) (u / u/rho)
S0	1.24	1.352 / 1.09	0.602 / 0.485	0.069 / 0.056	0.260 / 0.210
S1	1.67	1.278 / 0.765	0.569 / 0.341	0.050 / 0.030	0.261 / 0.156
S2	1.89	1.273 / 0.673	0.584 / 0.309	0.062 / 0.033	0.279 / 0.147
S3	2.1	1.271 / 0.605	0.541 / 0.257	0.071 / 0.034	0.296 / 0.141
S4	2.6	1.163 / 0.447	0.468 / 0.180	0.094 / 0.036	0.351 / 0.135

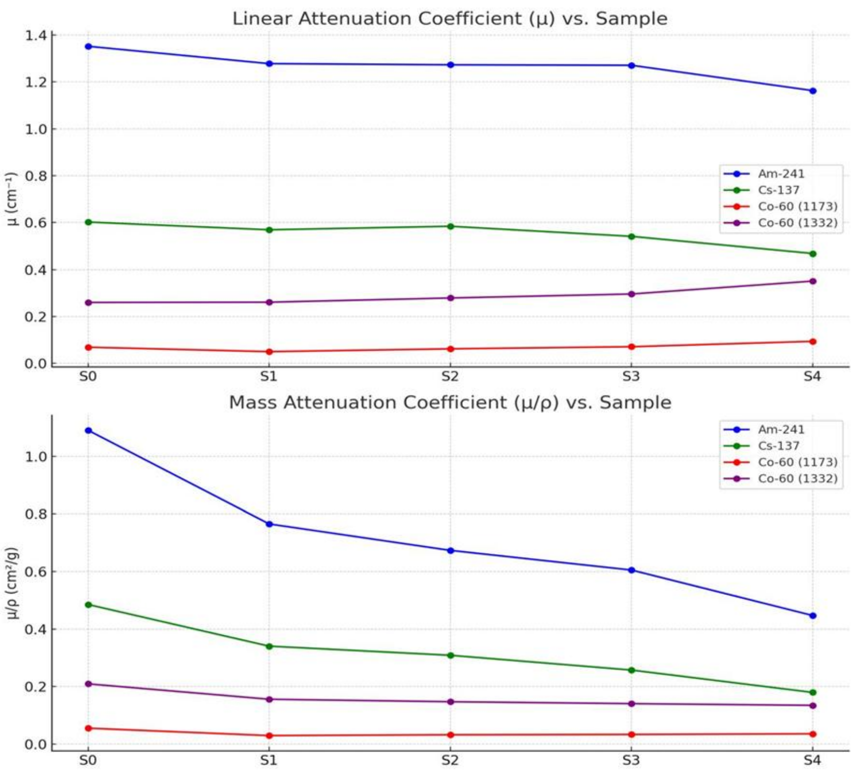

Fig. 2. Variation of linear and mass attenuation coefficients across samples with increasing densities under different radioactive sources.

(u/ρ) of five different samples (S0 to S4) with increasing density exposed to gamma radiation from four radioactive sources: Am-241, Cs-137, and Co-60 (1173 and 1332 keV).

Effect of Energy on Attenuation

An inverse relationship exists between photon energy and both attenuation coefficients. Am-241 (59.6 keV) consistently shows the highest u and u/ρ values across all the samples. As energy increases (Cs-137 at 661 keV and Co-60 at 1173 and 1332 keV), both coefficients decrease [15]. This finding is in line with the theory of gamma interaction with matter: The photoelectric effect is strongly dependent on atomic number (Z) dominates at low energies, leading to significant attenuation. At intermediate energies, Compton scattering becomes dominant, causing moderate attenuation. At high energies (>1 MeV), pair production becomes significant, though only in very dense materials.

Effect of Material Density (Sample Variation)

As the sample density increases from S0 (1.24 g/cm^3) to S4 (2.60 g/cm^3), the following patterns are observed: The mass attenuation coefficient (u/ρ) tends to decrease, indicating that increasing density alone is not always efficient for shielding enhancement (Fig. 2). The linear attenuation coefficient (u) slightly decreases or plateaus, especially for high-energy gamma-ray sources, due to the diminishing effect of added thickness on highly penetrating radiation [16].

.

CONCLUSION

The linear (u) and mass (u/ρ) attenuation coefficients of samples S0–S4 in the presence of gamma-ray sources Am-241, Cs-137, and Co-60 were analyzed. The following conclusions were drawn:

1- Low-energy gamma-ray sources (e.g., Am-241 at 59.6 keV) exhibit significantly higher attenuation coefficients than high-energy gamma-ray sources.

2- Photon energy is inversely related to linear and mass attenuation coefficients.

3- The mass attenuation coefficient (u/ρ) decreases with the increasing material density, indicating diminishing returns in shielding beyond certain density thresholds.

4- The linear attenuation coefficient (u) shows a plateau trend at high densities, especially for high-energy gamma-ray sources such as Co-60.

5- As a baseline, sample S0 provides a reference point for assessing the impact of increasing density in subsequent samples.

6- Effective gamma shielding design must consider photon energy and material properties (such as density and thickness).

7- The results align with expected radiation–matter interaction models: photoelectric effect, Compton scattering, and pair production.

8- For low-energy gamma-ray sources, increasing density significantly improves shielding. For high-energy radiation, material selection and total thickness are more crucial than density.

CONFLICT OF INTEREST

The authors declare that there is no conflict of interests regarding the publication of this manuscript.

REFERENCES

1. Gohel A, Makwana R. Multi-layered shielding materials for high energy space radiation. Radiat Phys Chem. 2022;197:110131.
2. Miza Osman N, Mohamad Tajudin S, Hanim Aminordin Sabri A, Faddilah Mohd Noor A, Zahri Abdul Aziz M. Evaluation of scattering effects for radiation shielding or filter materials by using Monte Carlo simulation. IOP Conference Series: Materials Science and Engineering. 2022;1231(1):012007.
3. Hubbell JH, Seltzer SM. Tables of x-ray mass attenuation coefficients and mass energy-absorption coefficients 1 keV to 20 MeV for elements Z = 1 to 92 and 48 additional substances of dosimetry interest. National Institute of Standards and Technology; 1995.
4. El-Kateb AH, Abdul-Hamid AS. Photon attenuation coefficient study of some materials containing hydrogen, carbon and oxygen. International Journal of Radiation Applications and Instrumentation Part A Applied Radiation and Isotopes. 1991;42(3):303-307.
5. Abouhaswa AS, El-Mallawany R, Rammah YS. Direct influence of La on structure, optical and gamma-ray shielding properties of lead borate glasses. Radiat Phys Chem. 2020;177:109085.
6. Wood J. TRANSPORT THEORY METHODS. Computational Methods in Reactor Shielding: Elsevier; 1982. p. 270-428.
7. London PS. Casualty officer’s handbook. D. H. Wilson and M. H. Hall. Fourth edition. 223 × 142 mm. Pp. 294 + vii. Illustrated. 1979. London: Butterworth. £9·95. Journal of British Surgery. 1980;67(5):379-379.
8. Advanced organic chemistry Third edition), by G. W. Wheland. Pp. xi + 871. John Wiley and Sons Inc., New York; John Wiley and Sons Ltd, London. 1960. E7 net. Endeavour. 1961;20(79):171.
9. Hawes C. Biology, 2nd edition N A Campbell, Benjamin/ Cummings Publishing Co. Inc. Cell Biol Int Rep. 1991;15(5):448-449.
10. Simmons JA. Physics for Radiation Protection. By J E Martin. pp. 844, 2006 (John Wiley and Sons, Inc,, Oxford,

UK) £135.00 ISBN 978-3527406111. The British Journal of Radiology. 2007;80(959):949-949.
11. Vanamala UM, Nidamarty LP. Galactic Cosmic Energy - A Novel Mode of Energy Harvesting. Learning and Analytics in Intelligent Systems: Springer International Publishing; 2019. p. 458-465. http://dx.doi.org/10.1007/978-3-030-24314-2_55
12. Georgiou CD, Kalaitzopoulou E, Skipitari M, Papadea P, Varemmenou A, Gavriil V, et al. Physical Differences between Man-Made and Cosmic Microwave Electromagnetic Radiation and Their Exposure Limits, and Radiofrequencies as Generators of Biotoxic Free Radicals. Radiation. 2022;2(4):285-302.
13. Cucinotta FA, Kim M-HY, Ren L. Evaluating shielding effectiveness for reducing space radiation cancer risks. Radiat Measur. 2006;41(9-10):1173-1185.
14. Fearn SJ, Kaluvan S, Scott TB, Martin PG. An Open-Source Iterative Python Module for the Automated Identification of Photopeaks in Photon Spectra. Radiation. 2022;2(2):193-214.
15. Torresan C, Benito Garzón M, O'Grady M, Robson TM, Picchi G, Panzacchi P, et al. A new generation of sensors and monitoring tools to support climate-smart forestry practices. Can J For Res. 2021;51(12):1751-1765.
16. Webber WR. Galactic Cosmic Rays from 1 MeV to 1 GeV as Measured by Voyager beyond the Heliopause. Cosmic Rays: InTech; 2018.